Applied Catalysis B: Environmental 140–141 (2013) 108–114

Contents lists available at SciVerse ScienceDirect

Applied Catalysis B: Environmental

journal homepage: www.elsevier.com/locate/apcatb

Cu-modified TiO_2 photocatalysts for decomposition of acetic acid with simultaneous formation of C_1–C_3 hydrocarbons and hydrogen

Aleksandra Heciak*, Antoni W. Morawski, Barbara Grzmil, Sylwia Mozia

West Pomeranian University of Technology, Szczecin, Institute of Chemical and Environment Engineering, ul. Pułaskiego 10, 70-322 Szczecin, Poland

ARTICLE INFO

Article history:
Received 3 January 2013
Received in revised form 18 March 2013
Accepted 27 March 2013
Available online 2 April 2013

Keywords:
Photocatalysis
Hydrocarbons
Hydrogen
Acetic acid
Cu/TiO_2

ABSTRACT

Three different methods of modification (impregnation, photodeposition and mechanical alloying) were used to obtain a series of novel Cu/TiO_2 photocatalysts. Two Cu(II) salts: $(Cu(NO_3)_2$ and $Cu(CH_3COO)_2)$ as well as metallic copper were applied as modifying agents. The influence of the modification procedure and copper precursor on the physico-chemical properties and photoactivity of the photocatalysts towards formation of useful hydrocarbons from acetic acid were especially investigated. Various gaseous products were identified during the photocatalytic process: CH_4, CO_2, C_2H_6, C_3H_8 and H_2. The amounts of those compounds were strongly dependent on the photocatalyst type. Crucial features affecting the photoactivity of the obtained materials were the amount of Cu and phase composition of the samples. Nonetheless, most of the Cu/TiO_2 photocatalysts revealed significantly improved activity in the photocatalytic generation of useful aliphatic hydrocarbons and hydrogen compared to the crude TiO_2 or commercial TiO_2 P25.

1. Introduction

For the past few decades, increased concern for emission of greenhouse gases and depletion of non-renewable resources contributed to the development of new methods of energy production, mainly from alternative sources, such as biomass. Conversion of waste and wastewaters into energy would be desirable from both ecological and economical point of view. One of the most promising and common method of energy production is transformation of organic substrates to biogas [1,2]. Biogas is a mixture of different gases, mainly methane and carbon dioxide. Its production during anaerobic digestion possesses some serious drawbacks. One of the most important relates to the sensitivity of methanogenic bacteria, which makes plenty of possible substrates excluded from the conventional technology of biogas production. Since photocatalysis is not selective for particular substances it could be a good alternative to the biological process and its limitations [3].

Titanium dioxide is known as one of the most active, stable and relatively cheap photocatalysts, therefore, is being widely used and investigated. However, efficiency of the photocatalytic reaction in the presence of TiO_2 is often low due to the fast recombination between photogenerated holes and electrons. In order to overcome the above problem, TiO_2 can be modified with various organic or inorganic substances. Among them, incorporation of metals, such as Fe, Pt, Ag and Cu or their oxides into the photocatalysts structure has attracted significant attention [4–10]. Metal-modified TiO_2 photocatalysts are well known for their improved photocatalytic activity which originates from the charge trapping and reduction of e^-/h^+ recombination rate [4].

Most papers concerning photocatalytic removal of organic contaminants from water focus on evaluation of solution composition in terms of liquid products and by-products formed during the photodegradation. The composition of gas phase in case of such processes has been explored much less extensively. However, the literature data show, that the gaseous phase might contain products of photodegradation which could be possibly utilized. Such a compound is e.g. methane formed during photodecomposition of acetic acid.

First reports related to the photocatalytic generation of hydrocarbons from organics in the gaseous phase were published in 1970s by Kraeutler and Bard [11–13]. They used Pt/TiO_2 photocatalysts for photocatalytic decarboxylation of acetic acid under UV light. The reaction in which CH_4 and CO_2 were evolved as the main products, was named the "photo-Kolbe reaction".

Recently, we have reported application of various pure and metal-modified TiO_2 photocatalysts in the reaction of acetic acid degradation [14–16]. We have proved that modification of titanium dioxide with iron by simple impregnation method can be a good way for improving the "photo-Kolbe reaction" efficiency.

The aim of this study was to evaluate the influence of modification procedure on the properties of new Cu/TiO_2 materials and their activity in the "photo-Kolbe reaction". The Cu-modified photocatalysts were prepared by three methods: impregnation, photodeposition or mechanical alloying. Moreover, various

* Corresponding author.
E-mail address: aheciak@zut.edu.pl (A. Heciak).

0926-3373/$ – see front matter © 2013 Elsevier B.V. All rights reserved.
http://dx.doi.org/10.1016/j.apcatb.2013.03.044

Cu-precursors such as $Cu(NO_3)_2$, $Cu(CH_3COO)_2$ or metallic copper were used. So far, most studies concerning Cu/TiO_2 application have been focused on either their photocatalytic activity towards CO_2 reduction [17–21] or hydrogen generation [5,7,9,22]. A possible utilization of Cu/TiO_2 in the photocatalytic formation of hydrocarbons, such as methane, from organic matter was investigated, if ever, much less extensively. Moreover, among these papers, there were very few attempts of comparing effects of application of various methods of TiO_2 modification with several copper ions precursors on the physico-chemical properties of the photocatalysts and photocatalytic reaction efficiency.

2. Experimental

2.1. Photocatalysts

Cu/TiO_2 photocatalysts were synthesized by three methods: impregnation (i), photodeposition (p) and mechanical alloying (ma), from a crude TiO_2 obtained directly from the production line (sulphate technology) at the Chemical Factory "Police" (Poland). The chemical composition of the crude TiO_2 was as follows: TiO_2 66.05 wt.%, H_2SO_4 2.60 wt.%, Fe 0.06 wt.%, Si 0.01 wt.%, Mg 0.04 wt.%, V 0.004 wt.%, Na 0.05 wt.% and the remaining was water (data from the manufacturer). As the copper precursors, copper(II) acetate ($Cu(CH_3COO)_2{\cdot}H_2O$) – denoted later as Ca, copper(II) nitrate ($Cu(NO_3)_2{\cdot}3H_2O$) – denoted as Cn and metallic copper (Cu) were used. The modified samples were named *x*-TiO_2-*y*, where *x* refers to the copper compound used and *y* to the modification procedure. Primarily, the copper content in the mixtures applied for the preparation of new materials varied from 5 to 20 wt.% with reference to the total mass of $Cu + TiO_2$. Photocatalysts were calcined at different temperatures ranging from 400 to 800 °C. From a series of the obtained materials, one sample, obtained by each technique, which exhibited the highest activity toward CH_4 generation, was selected and characterized in the present paper. Moreover, in order to compare the results, crude TiO_2 and commercially available photocatalyst AEROXIDE® P25 (Evonik, Germany) were applied in the photocatalytic experiments.

2.1.1. Impregnation (i)

A defined amount of dried crude TiO_2 was introduced into a beaker containing aqueous solution of $Cu(CH_3COO)_2$ or $Cu(NO_3)_2$ and stirred for 22 h (the amount of Cu with relation to the sum of $Cu + TiO_2$ was 10 wt.% in both cases). After that water was evaporated and the samples were dried at 80 °C for 24 h. Photocatalysts modified with $Cu(CH_3COO)_2$ or $Cu(NO_3)_2$ were then calcined at 500 and 600 °C, respectively, in Ar atmosphere (83 dm^3/min) for 1 h. Such prepared photocatalysts were named Ca-TiO_2-i and Cn-TiO_2-i, respectively.

2.1.2. Photodeposition (p)

A defined amount of dried crude TiO_2 was introduced into a cylindrical glass reactor (Heraeus, type UV-RS-2) containing aqueous solution of $Cu(CH_3COO)_2$ or $Cu(NO_3)_2$ (the amount of Cu with relation to the sum of $Cu + TiO_2$ was 10 wt.% in both cases). Moreover, small amount of methanol (1 mol/dm^3) was added as the sacrificial agent. The light source used was a medium pressure mercury vapour lamp (TQ-150, λ_{max} = 365 nm). The irradiation was conducted for 24 h in N_2 atmosphere. The reaction mixture was continuously stirred during the modification by means of a magnetic stirrer.

After the irradiation, the photocatalyst was washed with ultrapure water and centrifuged three times in order to remove the residual copper salt and methanol. Such prepared samples were dried and subsequently calcined for 1 h at 700 or 600 °C (Ar atmosphere, gas flow 83 dm^3/min) in case of prior using of $Cu(CH_3COO)_2$ or $Cu(NO_3)_2$ solution, respectively. The prepared photocatalysts were named Ca-TiO_2-p and Cn-TiO_2-p, respectively.

2.1.3. Mechanical alloying (ma)

A defined amount of dried crude TiO_2 and metallic copper powder was mechanically grounded for 12 h by a planetary ball mill (PM100, RETSCH). The ball-milling speed was 150 rpm. The copper content was 10 wt.% with relation to the sum of $Cu + TiO_2$. After the mechanical modification the sample was calcined at 500 °C in Ar atmosphere (83 dm^3/min) for 1 h. Such prepared photocatalyst was named Cu-TiO_2-ma.

2.2. Photocatalysts characterization

The photocatalysts were characterized by X-ray diffraction (XRD), UV–Vis/DR spectroscopy and N_2 adsorption at 77 K measurement. Moreover, X-ray fluorescence (XRF) was applied to determine Cu content in the obtained materials.

The XRD patterns were recorded using X'Pert PRO diffractometer with CuKα radiation (λ = 1.54056 Å). TiO_2 anatase over rutile ratio was calculated from [23]:

$$\text{Anatase content } A = \frac{1}{(1 + 1.26(I_R/I_A))} \quad (1)$$

where I_A and I_R are the diffraction intensities of the (1 0 1) anatase and (1 1 0) rutile crystalline phases at 2θ = 25.3 and 27.4°, respectively. The average anatase crystallite diameter D (nm) was calculated using Scherrer's equation [23,24]:

$$D = \frac{K\lambda}{\beta \cos\theta} \quad (2)$$

where K = 0.9 is a shape factor for spherical particles, λ is the wavelength of the incident radiation (λ = 1.54056 Å), θ is half of the diffraction angle (rad) and β is the line width at half-maximum height.

The UV–Vis/DR spectra were recorded using Jasco V530 spectrometer (Japan) equipped with the integrating sphere accessory for diffuse reflectance spectra. $BaSO_4$ was used as a reference.

The specific surface area (S_{BET}) of the photocatalysts was determined on a basis of N_2 adsorption isotherms measured at 77 K using Quadrasorb SI (Quantachrome Instruments) analyzer. Before measurement samples were dried and degassed at 150 °C for 24 h.

The amount of copper in the final Cu/TiO_2 photocatalysts was determined on a basis of energy dispersive X-ray fluorescence (EDXRF) measurement (Epsilon 3, PANalytical).

2.3. Photocatalytic reaction

The photocatalytic reaction was conducted in a closed cylindrical quartz reactor (Heraeus, type UV-RS-2). A medium pressure mercury vapour lamp (TQ-150, λ_{max} = 365 nm) located in the centre of the vessel was used as an irradiation source. The total volume of the reactor was 765 cm^3 (350 cm^3 and 415 cm^3 of a liquid and gaseous phase, respectively). In the upper part of the reactor a gas sampling port was mounted.

Considering that biomass is regarded as the most promising renewable energy resource, acetic acid was selected as a model biomass-derived compound. Furthermore, CH_3COOH undergoes the "photo-Kolbe reaction" which means that the gaseous mixture obtained during the photocatalytic reaction will have a composition similar to that of biogas produced in a conventional anaerobic digestion process.

At the beginning of each experiment 0.35 dm^3 of CH_3COOH (1 mol/dm^3) aqueous solution and 1 g/dm^3 of a photocatalyst were introduced into the reactor. Before the startup of the irradiation N_2 was bubbled through the reactor for at least 1 h in order to eliminate

Table 1
Physico-chemical properties of the crude TiO_2, P25 and Cu/TiO_2 photocatalysts: (A) anatase; (R) rutile; (*) excluding the amorphous phase.

Photocatalyst	Temperature of calcination (°C)	Cu source	Modification procedure	Anatase crystallite size (nm)	A:R ratio*	Phase composition	S_{BET} (m^2/g)
Crude TiO_2	–	–	–	7	85:15	A, R	215
P25	–	–	–	22	80:20	A, R	50
Ca-TiO_2-p	700	$Cu(CH_3COO)_2{\cdot}H_2O$	photodeposition	–	0:100	R, Cu_2O, CuO	10
Ca-TiO_2-i	500	$Cu(CH_3COO)_2{\cdot}H_2O$	impregnation	14	94:6	A, R, Cu	88
Cn-TiO_2-p	600	$Cu(NO_3)_3{\cdot}3H_2O$	photodeposition	62	88:12	A, R, CuO	10
Cn-TiO_2-i	600	$Cu(NO_3)_3{\cdot}3H_2O$	impregnation	45	91:9	A, R, $Cu_2O(SO_4)$, CuO	18
Cu-TiO_2-ma	500	metallic copper	mechanical alloying	29	93:7	A, R, CuO, Cu_2O	26

the dissolved oxygen. When the gas flow was stopped, the UV lamp was turned on to start the photoreaction. The process was conducted for 5 h. The reaction mixture containing the photocatalyst in the suspension was continuously stirred during the experiment by means of a magnetic stirrer. All the experiments were repeated at least twice in order to confirm the reproducibility of the results.

Gaseous products of the reaction were analyzed using GC SRI 8610 C equipped with TCD and HID detectors, and Shincarbon (carbon molecular sieve; 2 m, 1 mm, 100–120 mesh), molecular sieve 5A (3 m, 2 mm, 80–100 mesh) and 13X (1.8 m, 2 mm, 80–100 mesh) columns. Helium was used as the carrier gas. The composition of the liquid phase was determined using GC SRI 8610C equipped with FID detector and MXT®-1301 (60 m) column. Hydrogen was used as the carrier gas.

3. Results and discussion

3.1. Physico-chemical properties of the photocatalysts

Fig. 1 shows the XRD patterns of the TiO_2 and Cu/TiO_2 photocatalysts. The phase composition of the photocatalysts is presented in Table 1. The crude TiO_2 contained anatase and rutile phases in the ratio of 85:15. The diffraction lines were weak and broad suggesting poor crystallinity of the sample. The crystallite size of anatase in the crude TiO_2 was 7 nm.

The modification improved the crystalline structure of TiO_2, which resulted in narrowing and sharpening of the diffraction lines (Fig. 1). The samples calcined at 500–600 °C contained both anatase and rutile phases, regardless of Cu precursor. However, calcination at 700 °C led to a complete transformation of anatase to rutile (Ca-TiO_2-p). The crystallite size of anatase in case of the samples modified with copper was in the range of 14–62 nm (Table 1). The diameter of anatase crystallites was affected not only by the calcination temperature but also by the applied modification procedure. For example, Cn-TiO_2-p and Cn-TiO_2-i were both calcined at 600 °C but exhibited different anatase crystallite size (62 vs. 45 nm).

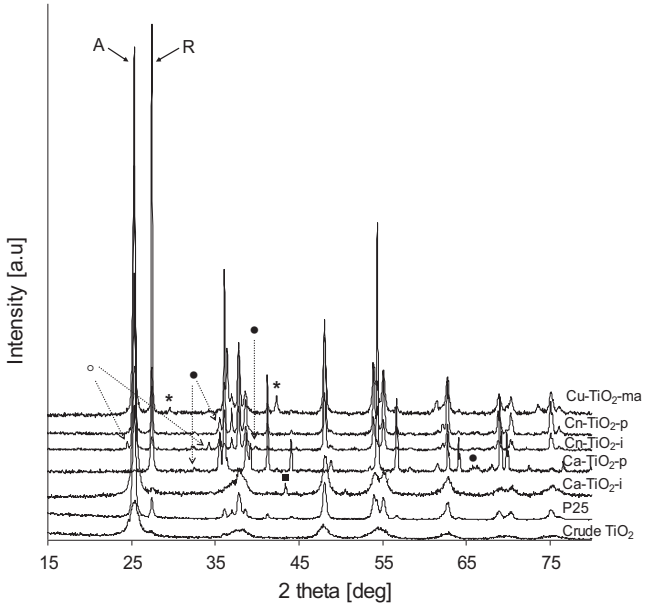

Fig. 1. XRD patterns of the crude TiO_2, P25 and Cu/TiO_2 photocatalysts: (A) anatase; (R) rutile; (●) CuO; (*) Cu_2O; (○) $Cu_2O(SO_4)$; (■) Cu.

The obtained data indicates that the phase composition of the materials obtained during modification with copper salts or metallic copper was changed: new phases appeared in case of Cu/TiO_2 photocatalysts (Table 1). TiO_2 can be simply doped with copper or the photocatalysts can be composed of mixtures of TiO_2 and copper oxide or oxides. Similarity of ionic radius of Cu^{2+} and Ti^{4+} (0.72 vs. 0.68 Å) promotes substitutional incorporation of modifying metal [10].

Detailed analysis of XRD patterns of the copper-modified photocatalysts revealed that CuO, Cu_2O, $Cu_2O(SO_4)$ and metallic Cu were present in the new materials. The existence of these phases in particular samples was dependent on the modification procedure and the applied modifying agent. In case of Ca-TiO_2-i photocatalyst metallic copper was identified besides anatase and rutile phases. The Cn-TiO_2-i contained CuO and $Cu_2O(SO_4)$, whereas the other samples consisted of either single or mixed oxides: CuO and Cu_2O. According to Francisco and Mastelaro [25], CuO creates a higher number of defects, most likely oxygen vacancies, in the TiO_2 crystals, accelerating the crystallite growth. That would be in agreement with our results since the photocatalysts containing CuO phase exhibited significantly higher size of anatase crystallites (Table 1) compared to Ca-TiO_2-i.

The crude TiO_2 was produced by the sulphate technology, thus contained some residual surface sulphates. At certain temperature (~600 °C) these species are usually thermally eliminated and rutilization process occurs [4,14]. Nonetheless, XRD patterns (Fig. 1) showed that in case of Cn-TiO_2-i even at 600 °C some sulphate groups were still present in the form of $Cu_2O(SO_4)$. That stabilization effect could be promoted by the presence of oxygen vacancies and, at lower temperatures, nitrate ions from the initial $Cu(NO_3)_2$ solution [4]. Moreover, both sulphate groups and oxygen vacancies stabilize the Cu_2O and CuO in the TiO_2 matrix [4]. Some of these conclusions were supported by the results obtained during the present investigation. In case of samples prepared from the copper(II) acetate, i.e. Ca-TiO_2-p or Ca-TiO_2-i (without nitrate or sulphate groups), transformation of anatase to rutile or CuO and Cu_2O into the metallic copper occurred, respectively.

Fig. 2 shows UV–Vis/DR spectra of pure TiO_2 and Cu/TiO_2. In general, the light absorption by the obtained materials was strongly affected by the presence of copper ions. For crude TiO_2 and P25 the absorption edges were 378 and 390 nm, respectively. In case of pure titania, the absorption is always associated with the O^{2-} (2p) → Ti^{4+} (3d) charge transfer process [4]. For Cu-modified photocatalysts, a great increase in the absorption at wavelengths longer than 400 nm was observed (Fig. 2). Moreover, a red shift of absorption edges which can be attributed to the presence of oxygen vacancies and/or

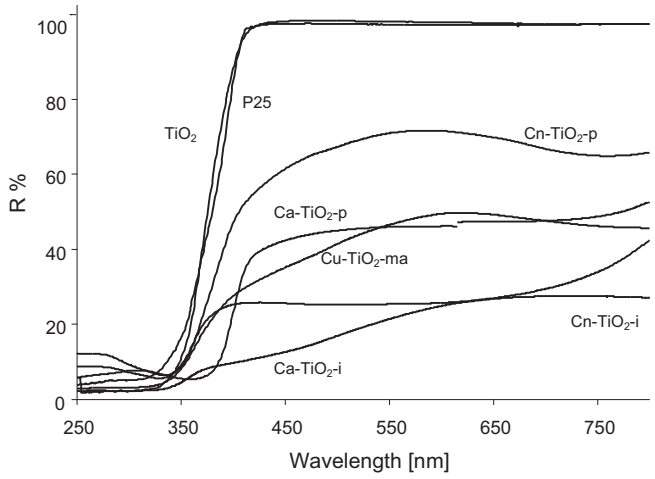

Fig. 2. UV–Vis/DR spectra of the crude TiO_2, P25 and Cu/TiO_2 photocatalysts.

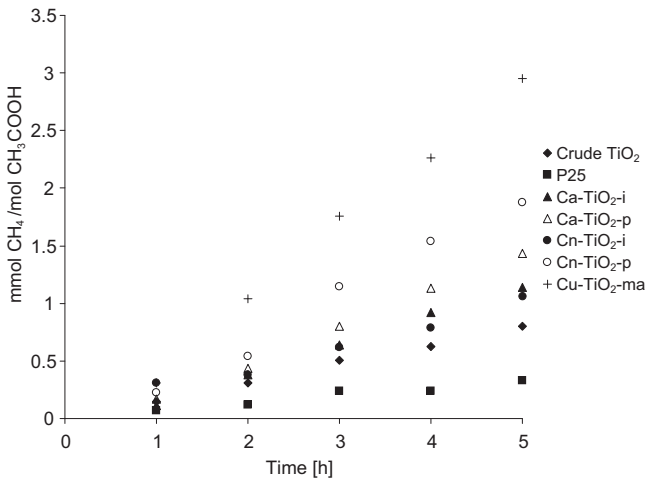

Fig. 3. Evolution of CH_4 in time of irradiation with application of crude TiO_2, P25 and Cu/TiO_2 photocatalysts. Photocatalyst loading: 1 g/dm^3; CH_3COOH concentration: 1 mol/dm^3; t = 25 °C; pH 2.6.

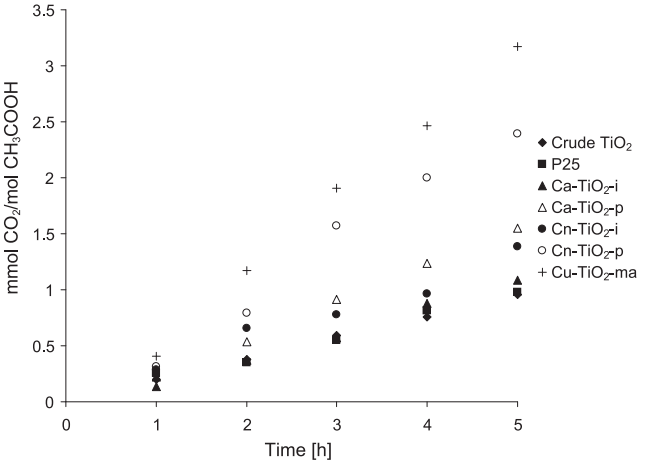

Fig. 4. Evolution of CO_2 in time of irradiation with application of crude TiO_2, P25 and Cu/TiO_2 photocatalysts. Photocatalyst loading: 1 g/dm^3; CH_3COOH concentration: 1 mol/dm^3; t = 25 °C; pH 2.6.

surface defects produced upon annealing correlated with a crystallization of the rutile phase can be seen [26]. This conclusion stays in agreement with the results obtained during XRD measurements (Fig. 1) which, in case of Cu/TiO_2, confirmed the appearance of rutile phase. Moreover, Cu_2O and CuO, present in the Cu-modified TiO_2, are p-type semiconductors with a small band gap energy. Thus, the absorption in the visible region (400–700 nm), characteristic of the Cu/TiO_2 (Fig. 2) could be also associated with the presence of these copper oxides in the photocatalysts structure [6].

The specific surface area (S_{BET}) of pure TiO_2 and Cu/TiO_2 is summarized in Table 1. It can be observed that the surface area of the crude titania was the highest (215 m^2/g). In case of Cu/TiO_2, the S_{BET} values were influenced by the temperature of annealing and decreased with increasing calcination temperature. The lowest S_{BET} was determined for the photocatalysts Ca-TiO_2-p, Cn-TiO_2-p and Cn-TiO_2-i calcined at 700 and 600 °C (10–18 m^2/g). It is worth mentioning, that the surface area of Cu/TiO_2 was also affected by the modification procedure. For instance, Ca-TiO_2-i and Cu-TiO_2-ma were both heat-treated at 500 °C, nonetheless, different techniques of modification and Cu precursor, entailed different values of S_{BET}.

In our previous report [14] we have proved that there is a strong correlation between the S_{BET} and anatase crystallites size. Similar dependence was observed in the present work. Diminishing S_{BET} of the Cu/TiO_2 resulted from dehydratation of TiO_2 and anatase crystals growth during annealing (Table 1) [14]. Moreover, Fig. 1 clearly indicates the growth of the CuO and Cu_2O crystals. This phenomenon contributed to the decrease of S_{BET} values in case of Cu-modified photocatalysts as well.

3.2. Photocatalytic activity

Crude TiO_2, commercially available P25 as well as the Cu/TiO_2 photocatalysts were applied in the photocatalytic decomposition of acetic acid under N_2 atmosphere. The identified gaseous products were CH_4, CO_2, C_2H_6, C_3H_8 and H_2. The presence and concentration of these compounds were dependent on the type of photocatalyst and its photoactivity. In all experiments, CH_4 and CO_2 were the main gaseous products of the photocatalytic reactions. All of the results presented below refer to the amount of C_1–C_3 hydrocarbons and H_2 evolved to the headspace volume of the reactor. Although the solubility of these gases in the liquid is not significant, their total concentrations were in fact higher than the measured ones, especially in case of CO_2. A detailed discussion concerning that phenomenon can be found in our previous paper [27].

Figs. 3 and 4 show the evolution of the main gaseous products (CH_4 and CO_2) as a function of irradiation time. After 5 h of the reaction the amounts of CH_4 and CO_2 were in the range of 0.33–2.95 mmolCH_4/molCH_3COOH and 0.96–3.17 mmolCO_2/molCH_3COOH, respectively. The highest evolution of both gases was observed in the presence of Cu-TiO_2-ma photocatalyst.

Among the gaseous products of the acetic acid decomposition, ethane, propane and hydrogen were also identified (Fig. 5). After

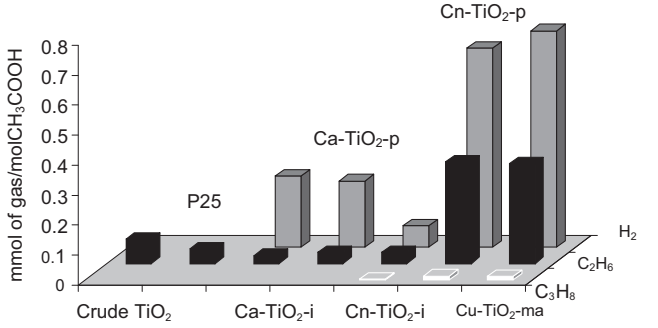

Fig. 5. Comparison of the amount of C_2H_6, C_3H_8 and H_2 evolved after 5 h in the presence of crude TiO_2, P25 and Cu/TiO_2 photocatalysts. Photocatalyst loading: 1 g/dm^3; CH_3COOH concentration: 1 mol/dm^3; t = 25 °C; pH 2.6.

5 h of the irradiation the amounts of C_2H_6, C_3H_8 and H_2 were in the range of 0.027–0.333 mmolC_2H_6/molCH_3COOH, 0–0.014 mmolC_3H_8/molCH_3COOH and 0–0.72 mmolH_2/molCH_3COOH. Once again, Cu-TiO_2-ma was one of the most efficient photocatalysts, which activity was comparable to the Cn-TiO_2-p, especially in case of propane and ethane generation. Therefore, on a basis of the presented data, it was proved that modification of TiO_2 with copper not only increased the amounts of gaseous products but also facilitated formation of H_2 and C_3H_8, unidentified in case of pure titania (crude TiO_2 and P25). The evolution of propane was, however, remarkably lower compared to CH_4 or CO_2.

An investigation on the composition of the liquid medium (acetic acid solution) after 5 h of the reaction revealed a presence of trace amounts of methanol (CH_3OH), ethanol (C_2H_5OH), acetone ($CO(CH_3)_2$)) and methyl acetate (CH_3COOCH_3). A detailed discussion on the mechanism of a photocatalytic decomposition of acetic acid and possible side reactions, including the formation of by-products in the liquid phase and mineralization of CH_3COOH, was already described elsewhere [15,16].

The obtained results (Figs. 3–5) clearly indicate that both, crude TiO_2 and commercially available P25, revealed minor photoactivity towards generation of all the gaseous products mentioned above compared to the Cu/TiO_2. In general, the effectiveness of the particular TiO_2 samples could be put in the following order: Cu-TiO_2-ma > Cn-TiO_2-p > Ca-TiO_2-p > Ca-TiO_2-i > Cn-TiO_2-i > crude TiO_2 > P25. Comparing these data with the specific surface area of the photocatalysts (Table 1) it could be concluded that S_{BET} did not influence the activity towards CH_4 formation. For example, Ca-TiO_2-p, with the same BET surface area as Cn-TiO_2-p (10 m^2/g), exhibited lower activity (Fig. 3). The highest surface area was determined for crude TiO_2 (215 m^2/g), however, it was significantly less effective than Cu-TiO_2-ma, which exhibited eight times lower S_{BET} value (26 m^2/g).

Another potentially important parameters are anatase over rutile ratio and crystallinity of the materials. Samples Ca-TiO_2-i and Cu-TiO_2-ma were characterized by a similar A:R ratio (94:6 vs. 93:7, respectively) but showed different effectiveness toward methane generation (Fig. 3). P25 had crystallites size of anatase similar to those characteristic of Cu-TiO_2-ma, however, it was significantly less active (Figs. 3–5). Moreover, at this point it is worth mentioning, that the sample Ca-TiO_2-p, which was composed of rutile only, was more efficient in CH_4 generation compared to the photocatalysts containing both anatase and rutile phases (e.g. Ca-TiO_2-i or pure TiO_2, Table 1, Fig. 3). It is somehow surprising since rutile is generally considered a poor photocatalyst. Its low activity is attributed to the rapid recombination of photogenerated electrons and holes (e^-/h^+) [28]. However, there are also some papers describing high photoactivity of rutile [29–31]. It should be also noted that, among the other things, rutile is chemically more stable than anatase, possesses a superior ability of light absorption, introduces mesoporosity and wider pore size distribution [32,33]. All that may contribute to its increased photocatalytic activity, in case of the present research as well.

Taking the above into consideration, neither S_{BET} nor anatase over rutile ratio and crystallite size of anatase, were found to be crucial properties responsible for the photocatalytic activity of the Cu/TiO_2 photocatalysts. Consequently, it was concluded that copper must have played an important role during the photocatalytic reaction.

According to the literature data [6,9,34] an improved activity of Cu/TiO_2 might be due to either one or a combination of the following factors: (a) increased light absorption; (b) effective capturing of the photoinduced electrons due to the appropriate amount of oxygen vacancies and Cu ions on TiO_2 surface. Copper ions can act as e^- traps to reduce the recombination rate of h^+/e^- pairs according to the following reactions [34]:

$$Cu^{2+} + e^- \rightarrow Cu^+ \quad (3)$$

$$Cu^+ + e^- \rightarrow Cu^0 \quad (4)$$

Therefore, both Cu^{2+} and Cu^+ ions are acceptors for the photogenerated electrons [33].

It is feasible in case of Cu^{2+} and Cu^+ to behave as the electron "traps" since they have more positive reduction potential than the conduction band edge of TiO_2 [33,34]. A result of capturing of e^- is better separation of h^+/e^- (therefore, improved holes availability), which explains higher photoactivity of Cu/TiO_2. The reduced state of copper (Cu^+/Cu^0), compared to Cu^{2+}, may limit electrons transfer from TiO_2, thus leading to a decrease of the reaction efficiency [9]. Moreover, acetic acid acts as a good hole scavenger, therefore, even greater separation of the photoinduced charges can be achieved [14–16]. This is associated with the fact that CH_3COOH degradation follows the so called "photo-Kolbe reaction" pathway initiated by the photogenerated holes [11–16]. Obviously, good h^+/e^- separation is desirable for its efficiency.

According to Xu and Schoonen [35] the conduction (CB) and valence (VB) band edges of TiO_2, Cu_2O and CuO are −0.29, −0.28, 0.46 and 2.91, 1.92, 2.16 eV vs. NHE, respectively. Fig. 6 illustrates the positions of the CB and VB of TiO_2, CuO and Cu_2O, and the possible mechanisms of the transfer of photogenerated electrons in the mixed oxides. Additionally, the idea of "the photo-Kolbe" reaction which involves the photogenerated h^+ is shown. Absorption of light having energy greater than the band gap (E_g) energies of TiO_2, CuO and Cu_2O results in photogeneration of holes in VB and electrons in CB of the semiconductors. Since conduction bands of both Cu_2O and CuO are situated below the CB of TiO_2, the electrons might be transferred from TiO_2 to Cu_2O (Fig. 6a) or CuO (Fig. 6b). In case of photocatalysts containing both Cu oxides, such as Cu-TiO_2-ma (Table 1) the mechanisms shown in Fig. 6c and d might also occur. In the Cu_2O/CuO composites the photogenerated e^- from Cu_2O might be easily injected to the conduction band of CuO (Fig. 6c). In case of TiO_2/Cu_2O/CuO photocatalysts the electrons from TiO_2 might additionally take part in this process (Fig. 6d). Consequently, the accumulation of excess electrons in CuO or/and Cu_2O conduction bands takes place. As a result, the lifetime of holes in VB of TiO_2 is prolonged. This influences positively on the efficiency of the "photo-Kolbe" reaction, in which h^+ are consumed by the CH_3COOH molecules. Meanwhile, the excess electrons in CB might react mainly with H^+ (under anaerobic conditions) to generate H_2 [36].

The mechanism discussed above is in a good agreement with our results since the photocatalysts containing CuO/Cu_2O or CuO phases (Table 1) where the most efficient in hydrocarbons, mainly CH_4, and hydrogen generation from CH_3COOH (Figs. 3 and 5). Ca-TiO_2-i containing only Cu^0, was one of the least effective photocatalysts among the Cu/TiO_2.

In general, the highest photoactivity was observed when mechanical alloying with metallic copper was used in order to modify crude TiO_2. The modification by the impregnation led to the formation of much less active materials due to the introduction of an inappropriate reduced state of copper ($^+/^0$) (Figs. 3–5).

Fig. 7 summarizes the influence of Cu/TiO_2 photocatalysts composition in terms of crystalline phases and Cu content on the effectiveness of CH_4 evolution. The amount of Cu with relation to Cu + TiO_2 used during modification was always 10 wt.%. Nonetheless, since the actual quantity of copper in the materials might be different from the initial value, depending on the applied modification technique, the Cu content was verified on a basis of XRF analysis. The measured amounts were 6, 10, 9, 10 and 10 wt.% for Ca-TiO_2-p, Ca-TiO_2-i, Cn-TiO_2-p, Cn-TiO_2-i and Cu-TiO_2-ma,

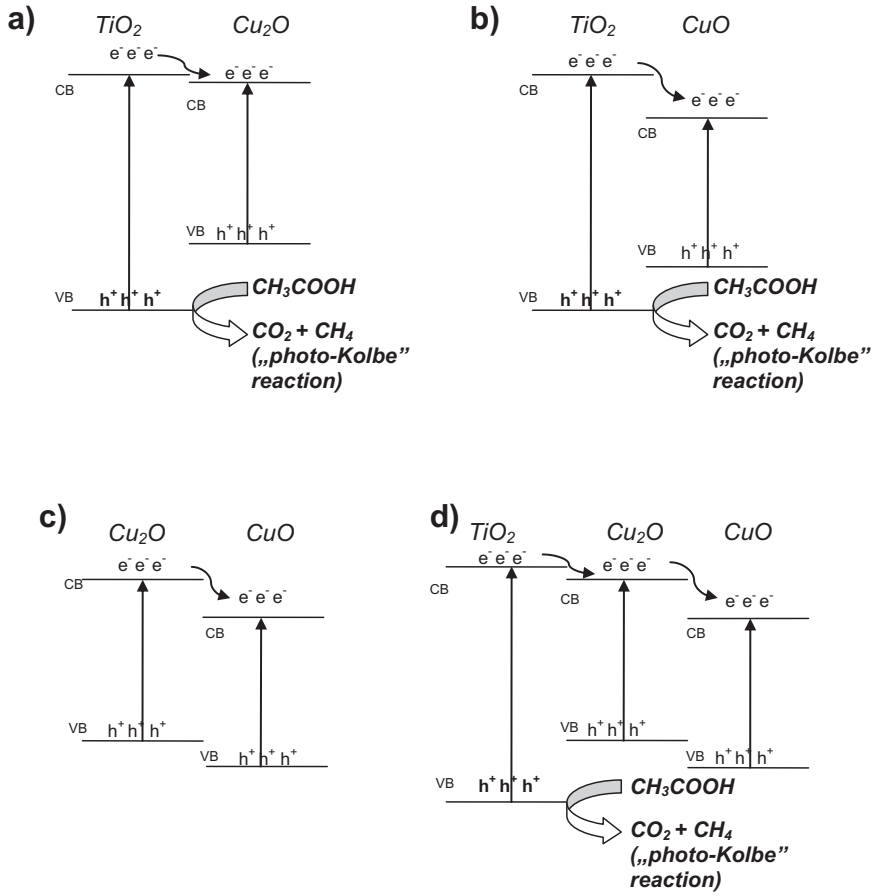

Fig. 6. Schematic diagrams of electron transfer under UV irradiation for Cu/TiO_2 photocatalysts: (CB) conduction band; (VB) valence band.

respectively. Fig. 7 indicates that the amount of Cu in the samples was not the only factor influencing their activity. It shows that another key parameter was phase composition of the photocatalysts. Amongst the samples containing 10 wt.% of Cu, i.e. Cn-TiO_2-i, Ca-TiO_2-i and Cu-TiO_2-ma, the latter one was the most active when methane formation is considered. According to the mechanism discussed earlier, the observed high efficiency of this material could be attributed to a presence of mixed (Cu_2O/CuO) copper oxides. The mechanism explains also lower activity of Cn-TiO_2-p, which contained CuO phase only. The Ca-TiO_2-i and Cn-TiO_2-i photocatalysts containing 10 wt.% of Cu, obtained by the impregnation method were the least efficient in the "photo-Kolbe" reaction among all the prepared samples. Their low activity could be explained by the presence of less preferable reduced state of copper (Cu^0) and mixed phases of CuO and $Cu_2O(SO_4)$. Furthermore, lower activity of Ca-TiO_2-p compared to Cu-TiO_2-ma resulted from both lower Cu content (6 wt.%) and transformation of anatase to rutile.

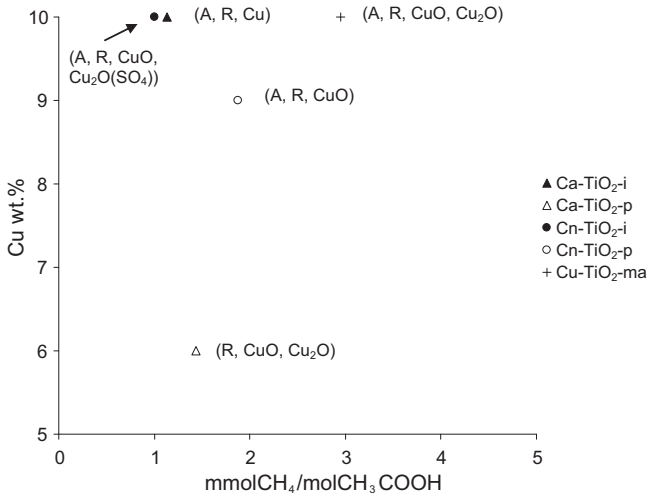

Fig. 7. Dependence between the effectiveness of the Cu/TiO_2 photocatalysts toward CH_4 evolution and the amount of copper and its state: (A) anatase; (R) rutile. Photocatalyst loading: 1 g/dm^3; CH_3COOH concentration: 1 mol/dm^3; t = 25 °C; pH 2.6.

4. Conclusions

Impregnation and photo-deposition methods as well as the mechanical alloying with application of $Cu(NO_3)_2$, $Cu(CH_3COO)_2$ or metallic copper were used in order to obtain Cu- modified TiO_2 photocatalysts with improved photoactivity in the photo-Kolbe reaction. The obtained results revealed, that the simplest technique – mechanical alloying with metallic copper followed by calcination allowed to synthesize the most efficient photocatalyst (Cu-TiO_2-ma) which might be beneficial, especially when the future larger-scale application is considered.

The high activity of Cu-TiO_2-ma towards hydrocarbons and hydrogen generation was attributed to the presence of an appropriate amount of copper in advantageous state of Cu ions – both Cu^{2+}/Cu^+. In the investigated reaction, CuO and Cu_2O act as the photogenerated electrons traps while CH_3COOH as the holes scavenger. Thus, the recombination rate of h^+/e^- decreases and the effectiveness of the Cu-modified photocatalysts is enhanced.

It was concluded that photocatalysts properties such as the anatase over rutile ratio, anatase crystallite size and specific surface area S_{BET} did not play a crucial role in the investigated process.

The obtained results proved that the Cu/TiO_2 can be applied for photocatalytic generation of useful C_1–C_3 hydrocarbons and hydrogen. Nonetheless, in order to determine the stability of the prepared photocatalysts against possible photocorrosion and application in other photocatalytic reactions, further investigations are necessary.

Acknowledgment

This work was supported by The National Science Center (Poland) under project No. 2011/01/N/ST5/02543.

References

[1] B. Demirel, P. Scherer, Renewable Energy 34 (2009) 2940–2945.
[2] M. Pöschl, S. Ward, P. Owende, Applied Energy 87 (2010) 3305–3321.
[3] K. Hanaki, S. Hirunmasuwan, T. Matsuo, Water Research 28 (1994) 877–885.
[4] G. Colón, M. Maicu, M.C. Hidalgo, J.A. Navío, Applied Catalysis B 67 (2006) 41–51.
[5] N.-L. Wu, M.-S. Lee, International Journal of Hydrogen Energy 29 (2004) 1601–1605.
[6] B. Xin, P. Wang, D. Ding, J. Liu, Z. Ren, H. Fu, Applied Surface Science 254 (2008) 2569–2574.
[7] M. Manzoli, A. Chiorino, F. Boccuzzi, Applied Catalysis B 57 (2004) 201–209.
[8] C. He, D. Shu, M. Su, D. Xia, M. Abou Asi, L. Lin, Y. Xiong, Desalination 253 (2010) 88–93.
[9] S. Xu, D.D. Sun, International Journal of Hydrogen Energy 34 (2009) 6096–6104.
[10] H.S. Park, D.H. Kim, S.J. Kim, K.S. Lee, Journal of Alloys and Compounds 415 (2006) 51–55.
[11] B. Kraeutler, A.J. Bard, Journal of the American Chemical Society 99 (1977) 7729–7731.
[12] B. Kraeutler, A.J. Bard, Journal of the American Chemical Society 100 (1978) 2239–2240.
[13] B. Kraeutler, C.D. Jaeger, A.J. Bard, Journal of the American Chemical Society 100 (1978) 4903–4905.
[14] S. Mozia, A. Heciak, A.W. Morawski, Applied Catalysis B 104 (2011) 21–29.
[15] S. Mozia, A. Heciak, A.W. Morawski, Catalysis Today 161 (2011) 189–195.
[16] S. Mozia, A. Heciak, A.W. Morawski, Journal of Photochemistry and Photobiology A 216 (2010) 275–282.
[17] I.H. Tseng, J.C.S. Wu, Catalysis Today 97 (2004) 113–119.
[18] Slamet, H.W. Nasution, E. Purnama, S. Kosela, J. Gunlazuardi, Catalysis Communications 6 (2005) 313–319.
[19] P.L. Richardson, M.L.N. Perdigoto, W. Wang, R.J.G. Lopes, Applied Catalysis B 126 (2012) 200–207.
[20] D. Liu, Y. Fernández, O. Ola, S. Mackintosh, M. Maroto-Valer, C.M.A. Parlett, A.F. Lee, J.C.S. Wu, Catalysis Communications 25 (2012) 78–82.
[21] D. Luo, Y. Bi, W. Kan, N. Zhang, S. Hong, Journal of Molecular Structure 994 (2011) 325–331.
[22] S. Xu, J. Ng, X. Zhang, H. Bai, D.D. Sun, International Journal of Hydrogen Energy 35 (2010) 5254–5261.
[23] G. Colón, J.M. Sánchez-España, M.C. Hidalgo, J.A. Navío, Journal of Photochemistry and Photobiology A 179 (2006) 20–27.
[24] K. Demeestere, J. Dewulf, T. Ohno, P. Herrera Salgado, H. Van Langenhove, Applied Catalysis B 61 (2005) 140–149.
[25] M.S.P. Francisco, V.R. Mastelaro, Chemistry of Materials 14 (2002) 2514–2518.
[26] S.K.S. Patel, N.S. Gajbhiye, Materials Chemistry and Physics 132 (2012) 175–179.
[27] S. Mozia, A. Heciak, D. Darowna, A.W. Morawski, Journal of Photochemistry and Photobiology A 236 (2012) 48–53.
[28] S. Sakthivel, M.C. Hidalgo, D.W. Bahnemann, S.U. Geissen, V. Murugesan, A. Vogelpohl, Applied Catalysis B 63 (2005) 31–40.
[29] B. Cao, L. Yao, C. Wang, X. Ma, X. Feng, X. Lu, Materials Letters 64 (2010) 1821–1919.
[30] J. Orlikowski, B. Tryba, J. Ziebro, A.W. Morawski, J. Przepiórki, Catalysis Communications 24 (2012) 5–10.
[31] D. Dolat, D. Moszyński, N. Guskos, B. Ohtani, A.W. Morawski, Applied Surface Science 266 (2013) 410–419.
[32] R.R. Bacsa, J. Kiwi, Applied Catalysis B 16 (1998) 19–29.
[33] A. Maurya, P. Chauhan, S.K. Mishra, R.K. Srivastava, Journal of Alloys and Compounds 509 (2011) 8433–8440.
[34] M. Hamadanian, A. Reisi-Vanani, A. Majedi, Applied Surface Science 256 (2010) 1837–1844.
[35] Y. Xu, M.A.A. Schoonen, American Mineralogist 85 (2000) 543–556.
[36] S. Xu, A.J. Du, J. Liu, J. Ng, D.D. Sun, International Journal of Hydrogen Energy 36 (2011) 6560–6568.